Finite element modelling of hybrid active–passive vibration damping of multilayer piezoelectric sandwich beams-part II: System analysis

Marcelo A. Trindade, Ayech Benjeddou, Roger Ohayon

Finite element modelling of hybrid active–passive vibration damping of multilayer piezoelectric sandwich beams—part II: System analysis

M. A. Trindade*†, A. Benjeddou and R. Ohayon

Structural Mechanics and Coupled Systems Laboratory,

Conservatoire National des Arts et Métiers, 2 rue Conté, 75003 Paris, France

An electromechanically coupled finite element model has been presented in Part 1 of this paper in order to handle active–passive damped multilayer sandwich beams, consisting of a viscoelastic core sandwiched between layered piezoelectric faces. Its validation is achieved, in the present part, through modal analysis comparisons with numerical and experimental results found in the literature. After its validation, the new finite element is applied to the constrained optimal control of a sandwich cantilever beam with viscoelastic core through a pair of attached piezoelectric actuators. The hybrid damping performance of this five-layer configuration is studied under viscoelastic layer thickness and actuator length variations. It is shown that hybrid active–passive damping allows to increase damping of some selected modes while preventing instability of uncontrolled ones and that modal damping distribution can be optimized by proper choice of the viscoel astic material thickness.

KEY WORDS: finite element; multilayer sandwich beam; piezoelectric material; viscoelastic material; active–passive vibration damping

INTRODUCTION

The model presented in Part 1 of this paper [1], using a finite element modelling associated with the anelastic displacement fields (ADF) viscoelastic model and a linear state-space feedback control law, has led to the following control system:

$$\dot{\hat{\mathbf{x}}} = (\hat{\mathbf{A}} - \hat{\mathbf{B}}\mathbf{K}_g)\hat{\mathbf{x}} + \hat{\mathbf{p}}, \quad \mathbf{y} = \hat{\mathbf{C}}\hat{\mathbf{x}} \tag{1}$$

where $\hat{\mathbf{A}}$, $\hat{\mathbf{B}}$ and $\hat{\mathbf{p}}$ are the system dynamics, input distribution and perturbation matrices, respectively, of the state-space modal reduced system. The measured variables $\mathbf{y}$ are written

*Correspondence to: M. A. Trindade, Structural Mechanics and Coupled Systems Laboratory, Conservatoire National des Arts et Métiers, 2 rue Conté, 75003 Paris, France
† E-mail: trindade@cnam.fr

Contract/grant sponsor: Délégation Générale pour l'Armement; contract/grant number: D.G.A./D.S.P./S.T.T.C/MA. 97-2530
Contract/grant sponsor: CAPES; contract/grant number: BEX 2494/95-7

in terms of the reduced state vector $\hat{\mathbf{x}}$ through the reduced matrix $\hat{\mathbf{C}}$. It should be noticed that the use of ADF viscoelastic model has led to a linear system with constant matrices but able to represent the frequency-dependence of the viscoelastic material. The problem of system dimension increase due to additional variables introduced by the ADF model was solved through a complex-based modal reduction of the state-space system. The feedback control gain matrix $\mathbf{K}_g$ is computed using an iterative linear quadratic regulator (LQR) optimal control algorithm [4] with weight matrices $\mathbf{Q}$ and $\mathbf{R} = \gamma\mathbf{I}$, γ being evaluated to respect maximum beam deflection and control voltage applied to the actuators.

In this part of the paper, the two-node sandwich piezo–visco–elastic finite element model with layered faces is first validated through comparisons with analytical, numerical and experimental results found in the literature. Then, the performance of the above hybrid active–passive control system is evaluated through the active control of a viscoelastically damped cantilever sandwich beam.

MODEL VALIDATION

The validation of the piezo–visco–elastic finite element model presented in Part 1 of this paper [1] will be carried out through the analysis of three examples: a laminate elastic/adhesive/piezoelectric beam, to validate the piezoelectric stiffness augmentation due to the induced potential; a 4 plies laminate composite beam, for the validation of the multilayer characteristic of the model, and a sandwich damped beam with bonded piezoelectric actuators, for a global validation of the piezo–visco–elastic model.

Piezoelectric layer bonded to a Timoshenko beam

As a first example, let us consider a cantilever sandwich beam made of aluminium with thickness 15.24 mm, width 25.4 mm and length 152.4 mm completely covered by a piezoelectric layer 10 times thinner. The two layers are bonded by an adhesive layer of thickness 0.254 mm (Figure 1). Material properties are given in Table I.

The first five eigenfrequencies are evaluated for two situations: open- and closed-circuit on the piezoelectric layer. For closed-circuit condition, the voltage in the piezoelectric layer vanishes, therefore its stiffness has only mechanical contributions. For open-circuit condition, the deformation of the sandwich beam induces a voltage in the piezoelectric layer, leading to an additional induced deformation of this layer. Notice that this could also be accounted for through a piezoelectric passive contribution to the layer stiffness (see Reference [1], Equation (31)). Present finite element results, using 15 elements, are compared to those given by Krommer and Irschik [2] and shown in Table II. PT and AB state for the Timoshenko multilayer theoretical and Abaqus finite element results presented in Reference [2]. The results

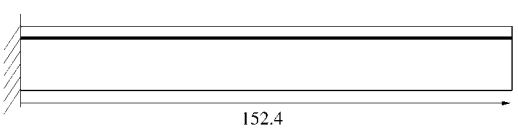

Figure 1. Timoshenko beam with a bonded piezoelectric layer (dimensions in mm).

Table I. Material properties for the cantilever Timoshenko sandwich beam.

	Aluminium	Piezoelectric	Adhesive
Elastic modulus (GPa), e_{11}^*	68.97	68.97	6.90
Shear modulus (GPa), c_{55}	27.59	—	—
Density ($\mathrm{kg\,m^{-3}}$), ρ	2769	7600	1662
Piezoelectric constant ($\mathrm{C\,m^{-2}}$), e_{31}^*	—	−8.41	—
Dielectric constant ($\mathrm{F\,m^{-1}}$), ε_{33}^*	—	1.15×10^{-8}	—

Table II. First five eigenfrequencies (Hz) of the cantilever Timoshenko sandwich beam.

	1	2	3	4	5
Closed circuit					
SH [3]	538.10	3199.00	7580.00	8350.00	15039.00
PT [2]	538.60	3211.00	7580.30	8394.86	15139.53
AB [2]	539.60	3200.40	7584.70	8326.70	14922.00
FEM	538.43	3206.67	7584.04	8388.22	15143.26
Error (%)	0.06	0.24	0.05	0.46	0.69
Open circuit					
SH [3]	544.10	3232.00	7614.00	8428.00	15167.00
PT [2]	544.10	3241.79	7611.03	8469.41	15262.68
AB [2]	543.81	3223.30	7608.70	8378.90	15004.00
FEM	543.34	3234.35	7613.47	8454.78	15252.56
Error (%)	−0.14	0.07	−0.01	0.32	0.56

found using the layerwise theory of Saravanos and Heyliger [3], which are able to reflect a non-linear distribution of axial displacements and electric potentials through division of piezoelectric layers in multiple sublayers, have been considered as the reference results (SH). Table II also shows the present results (FEM) error relative to the reference ones (SH). One may notice that present finite element results match well with previous theoretical and numerical results for both open- and closed-circuit conditions of piezoelectric layers.

Laminate composite beam

To validate the faces multilayer characteristic of the model, a modal analysis of laminate composite beams is performed and its results are compared to those presented in Reference [4]. Clamped–free (CL), clamped–simply supported (CS) and clamped–clamped (CC) 4 plies symmetric laminate beams $(0/90)_s$, made of three composite materials, namely Kevlar 49-epoxy, AS4/3501-6 and T300/N5208, are considered. The material properties are presented in Table III. All plies have the same thickness, the sum of which is denoted as $h = L/120$, length $L = 762\,\mathrm{mm}$ and width $b = L/15$.

It can be seen, in Table IV, that the first three eigenfrequencies of the laminate composite beams, using 20 elements of the present finite element model (sandwich/classical laminate theory, SCLT), match well with those presented in Reference [4], using first-order shear deformation theory (FSDT). One may also see that the model accuracy increases for stiffer

Table III. Material properties for the laminate composite beam.

	E_1	$E_2 = E_3$	$G_{12} = G_{13}$	G_{23}	$\nu_{12} = \nu_{13}$	ν_{23}	ρ
Kevlar 49-epoxy	76.0 GPa	5.56 GPa	2.30 GPa	1.60 GPa	0.34	0.7	1460 kg m^{-3}
AS4/3501-6	144.8 GPa	9.65 GPa	4.14 GPa	3.45 GPa	0.30	0.4	1389 kg m^{-3}
T300/N5208	181.0 GPa	10.3 GPa	7.17 GPa	3.40 GPa	0.28	0.5	1600 kg m^{-3}

Table IV. Comparison of first three bending non-dimensional eigenfrequencies ($= \omega L^2 \ (\rho/E_1 h^2)^{1/2}$) of a 4 plies symmetric $(0/90)_s$ laminate composite beam ($L/h = 120$).

	Kevlar 49-epoxy			AS4/3501-6			T300/N5208		
	CF	CS	CC	CF	CS	CC	CF	CS	CC
1(FSDT)	0.954	4.171	6.037	0.954	4.170	6.035	0.953	4.168	6.035
1(SCLT)	0.958	4.203	6.099	0.957	4.196	6.088	0.955	4.190	6.079
2(FSDT)	5.957	13.45	16.52	5.955	13.44	16.52	5.954	13.45	16.53
2(SCLT)	6.006	13.62	16.81	5.996	13.60	16.78	5.987	13.58	16.76
3(FSDT)	16.59	27.84	32.10	16.59	27.84	32.09	16.59	27.87	32.15
3(SCLT)	16.81	28.41	32.95	16.79	28.36	32.89	16.76	28.32	32.85

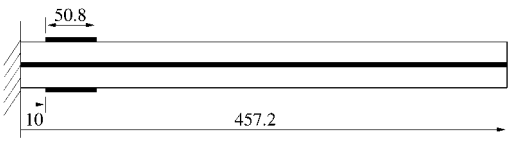

Figure 2. Cantilever sandwich beam with bonded actuators (dimensions in mm).

(T300/N5208) and less constrained (clamped–free) beams, since in these cases less shear is produced by deflection.

It is well known that classical laminate theory leads only to first approximations for cross-ply laminate composite beams. However, since most of the applications of the present sandwich beam model consists of stiff laminate faces and less stiff cores, it is assumed that most of the shear deformation will be performed by the core.

Sandwich damped beam with bonded actuators

Experimental validation was carried out through comparison with results presented by Wang and Wereley [5]. In this case, a sandwich cantilever beam, made of aluminium faces and ISD112 viscoelastic core, with a symmetrically attached pair of PZT5H piezoelectric patches is considered (Figure 2). Material and geometrical properties, adapted from Reference [5], are shown in Table V.

The 3M ISD112 viscoelastic material is modelled using three ADF, which parameters, evaluated from material master curves curve-fitting and valid, at 27°C, for the frequency range 20–5000 Hz, are $G_0 = 0.50$ MPa, $\Delta = [0.646, 3.265, 43.284]$ and $\Omega = [468.7, 4742.4, 71532.5]$ rad/s. The first three bending modes, represented in Figure 3, and corresponding eigen-frequencies

Table V. Material and geometrical properties of the five-layer beam of Reference [5].

	Aluminium	PZT5H	ISD112
Elastic modulus (GPa), c_{11}^*	75.8	68.1	Various
Density ($\mathrm{kg\,m^{-3}}$), ρ	2800	7500	1600
Piezoelectric constant ($\mathrm{C\,m^{-2}}$), e_{31}^*	—	−23.2	—
Dielectric constant ($\mathrm{F\,m^{-1}}$), ε_{33}^*	—	1.54×10^{-8}	—
Length (mm)	457.2	50.8	457.2
Thickness (mm)	0.794	0.254	0.254/0.127/0.051
Width (mm)	25.4	25.4	25.4

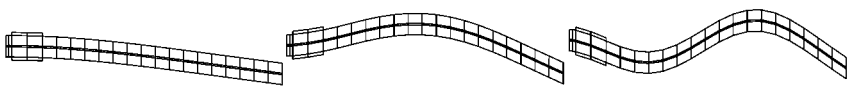

Figure 3. First three natural bending modes of the five-layer beam of Reference [5].

Table VI. Three first bending eigenfrequencies of the five-layer beam of Reference [5].

Mode	Experimental [5] Freq. (Hz)	PWM [5]		FEM	
		Freq. (Hz)	Error (%)	Freq. (Hz)	Error (%)
0.051 mm viscoelastic core					
1	6.64	6.37	−4.07	6.90	3.92
2	36.21	37.88	4.61	39.27	8.45
3	85.23	102.33	20.06	103.30	21.20
0.127 mm viscoelastic core					
1	6.84	6.69	−2.19	7.05	3.07
2	35.62	37.40	5.00	36.62	2.81
3	92.42	96.13	4.01	92.25	−0.00
0.254 mm viscoelastic core					
1	7.22	7.00	−3.05	7.30	1.11
2	36.79	36.76	−0.00	34.62	−5.90
3	89.50	89.60	0.11	84.66	−5.41

are then evaluated for each viscoelastic core thickness. Our finite element results, using 20 elements, are then compared to numerical ones, carried out using the progressive wave method (PWM), which accounts for frequency-dependent viscoelastic properties, and experimental ones presented in Reference [5]. Present results, shown in Table VI, match quite well with both experimental and numerical ones. It should be noticed that, for the thinner viscoelastic core configuration, our results are acceptable except for the third bending eigenfrequency which presents a large error of 21.20 per cent. However, it can be seen that the PWM leads to a similar error (20.06 per cent). This suggests that this reference value (experimental) may be not well measured.

Table VII. Material and geometrical properties of the sandwich damped beam with bonded piezoelectric actuators.

	Aluminium	PZT5H	ISD112
Elastic modulus (GPa), c_{11}^*	79.8	65.5	Various
Density ($\mathrm{kg\,m^{-3}}$), ρ	2690	7500	1600
Piezoelectric constant ($\mathrm{C\,m^{-2}}$), e_{31}^*	—	−23.2	—
Dielectric constant ($\mathrm{F\,m^{-1}}$), ε_{33}^*	—	1.54×10^{-8}	—
Length (mm)	250	50	250
Thickness (mm)	1.5	0.5	0.25
Width (mm)	25	25	25

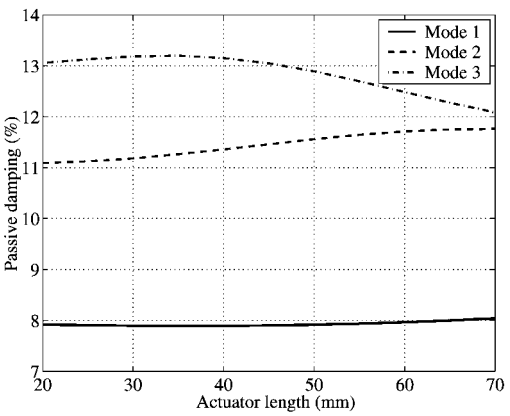

Figure 4. Three first bending modes passive damping vs. actuator length ($h_v = 0.25\,\mathrm{mm}$).

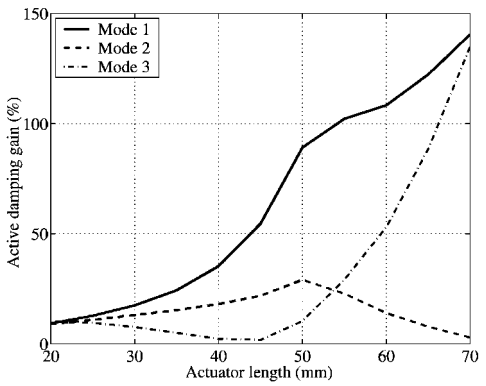

Figure 5. Three first bending modes active damping gain vs. actuator length ($h_v = 0.25\,\mathrm{mm}$).

HYBRID DAMPING PERFORMANCE

In this section, the finite element model, validated in the previous section, is used for the control synthesis and analysis of a cantilever sandwich damped beam treated by bonded piezoelectric actuators similar to that studied in the validation section (Figure 2), material and geometric properties of which are shown in Table VII. The control strategy presented in Part 1 [1] is considered, using the LQR iterative algorithm and supposing that the full state is measured. The weight matrix $\mathbf{Q}$ is considered to be diagonal and composed of the first three eigenfrequencies so that $\mathbf{Q} = \mathrm{diag}(\omega_1^2, \omega_2^2, \omega_3^2, 0, 0, 1, 1, 1, 0, 0)$ to maximize the damping of the energy of these first modes. For the example treated in what follows, the output $\mathbf{y}$ is taken to be the cantilever sandwich beam tip deflection and a perturbation transversal force applied at $x = 100\,\mathrm{mm}$ is considered. Voltages applied to the piezoelectric actuators are such that the maximum electrical field of $500\,\mathrm{V/mm}$ is not exceeded.

Furthermore, analysis of the variation, with the actuator length and damping core thickness, of passive damping, supplied by the viscoelastic damping layer, and corresponding damping gain relative to the passive one, developed by the piezoelectric feedback control, is carried

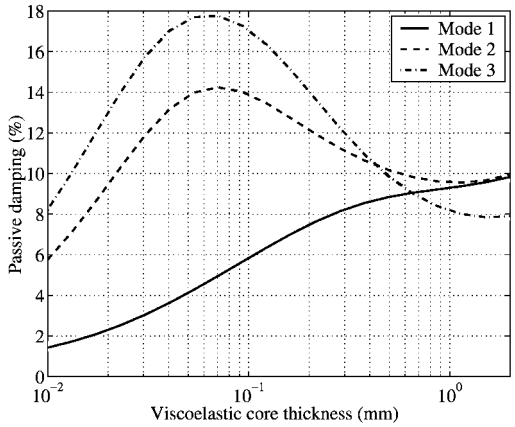

Figure 6. Three first bending modes passive damping vs. viscoelastic layer thickness ($a = 50\,\text{mm}$).

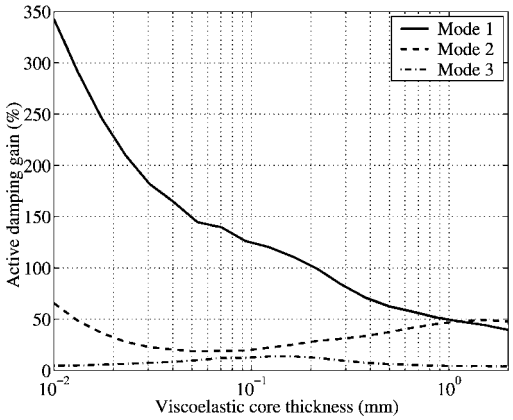

Figure 7. Three first bending modes active damping gain vs. viscoelastic thickness ($a = 50\,\text{mm}$).

out. First, the upper and lower piezoelectric actuators lengths are set to vary in the range 20–70 mm. As it can be seen in Figure 4, the actuator length variation does not affect much the passive viscoelastic damping, although one can notice a little overall augmentation, since only a face stiffening effect due to the piezoelectric layers is obtained. However, the active damping provided by the piezoelectric actuators increases greatly with their length (Figure 5). The first and third eigenmodes damping are augmented up to 140 per cent with respect to the passive one, for the longest actuators. Nevertheless, the second modal damping does not ameliorate that much.

Additionally, the viscoelastic core thickness is set to vary in the range 0.01–2 mm for a fixed actuator length of 50 mm. As it can be seen in Figure 6, the damping ratio of first mode is greater for increasing thickness, as was also shown numerically by van Nostrand and Inman [6]. However, for the second and third modes, modal dampings are optimal for relatively thin cores (around 0.06 mm). Although increasing viscoelastic material thickness may produce more passive damping, it also reduces the transmissibility between each actuator and its opposite elastic face, as reported in Reference [6]. This is the reason for the decrease in the hybrid damping performance for the first mode with increasing core thickness, as seen in Figure 7. Nevertheless, for the second mode, the effect is the opposite, that is, for its low passive damping range, active damping compensates, but does not surpass, the global damping of the sandwich beam. It is also clear that, as the controller loses its control performance for the first mode, it improves the second mode damping.

The previous results show that the active damping performance is improved for long actuators and thin cores, however in order to guarantee enough passive damping for the three modes, the viscoelastic core thickness is set to 0.06 mm. For these parameters, open- and closed-loop perturbation impulse responses of the sandwich beam tip deflection ($\mathbf{y}/\hat{\mathbf{p}}$) are shown, in the frequency and time domains, in Figures 8 and 9. From the frequency response function (Figure 8), one may notice that the first and third modes are greatly damped by the piezoelectric actuation, whereas the other modes damping remains almost constant. This is

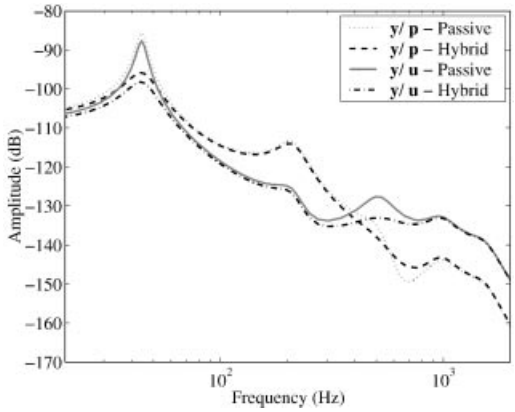

Figure 8. Frequency response function of the sandwich damped beam tip deflection ($a = 70\,\text{mm},\ h_v = 0.06\,\text{mm}$).

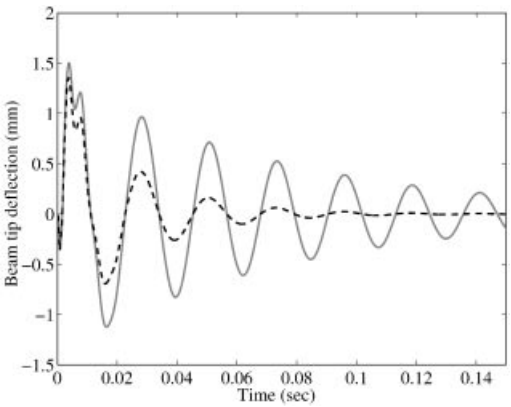

Figure 9. Impulse response of the sandwich damped beam tip deflection ($a = 70\,\text{mm},\ h_v = 0.06\,\text{mm}$).

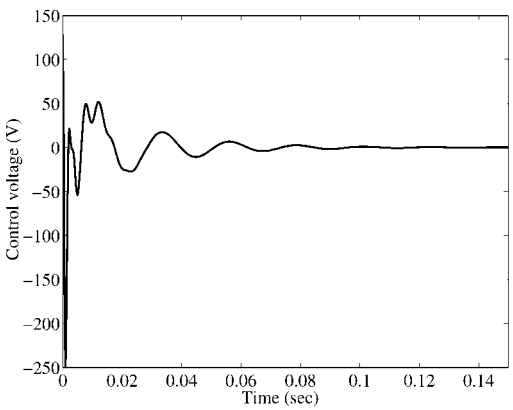

Figure 10. Actuator voltage needed to control impulse loaded sandwich beam ($a = 70\,\text{mm},\ h_v = 0.06\,\text{mm}$).

justified by the choice of the state ponderation, that is the choice of the elements of matrix **Q**, in the control design. Nevertheless, combination of passive and active damping not only allows to increase the damping of some selected modes but also guarantees some passive damping for uncontrolled modes. Furthermore, passive damping may prevent spillover effects. The frequency response function of the sandwich beam, when excited by the actuators (**y**/**u**), is also presented in Figure 8 and shows that the third mode resonance is almost cancelled.

For some applications, it is also necessary to analyse the transient response of the sandwich beam. Using the time-domain ADF viscoelastic modelling, this analysis is direct since all state-space matrices are frequency independent. Figure 9 shows the beam tip deflection impulse responses for open- and closed-loop situations. One may notice that output is quickly damped.

The actuator voltage needed for such performance, shown in Figure 10, is clearly limited by the input constraint of 250 V considered in the control algorithm.

CONCLUSIONS

The validation of the electromechanically coupled finite element model, presented in Part 1 of this paper [1], for the analysis of active–passive damped multilayer sandwich beams, was carried out through the analysis of three examples: a laminate elastic/adhesive/piezoelectric beam, a laminate composite beam and a sandwich damped beam with bonded piezoelectric actuators.

Present finite element results for modal analysis of the laminate elastic/adhesive/piezoelectric beam, under open- and closed-circuit conditions, match well with finite element and analytical results found in the literature. Modal analysis of laminate composite beams was performed to evaluate the accuracy of the classical laminate theory used for the faces. Its results were then compared to numerical ones, using first-order shear deformation theory, found in the literature and they matched well. Nevertheless, accounting for the shear strain in each piezoelectric layer was not considered but is being considered as future work. Furthermore, comparison of modal analysis results for a five-layer damped beam with experimental results found in the literature showed that the present model provides a good representation of both laminate/sandwich behaviour and viscoelastic material properties frequency-dependence. The numerical results indicate that the present finite element model leads to a simple but effective representation of the behaviour of multilayers active–passive constructions. The latter example was then considered for the analysis of the hybrid damping performance under viscoelastic layer thickness and actuators length variations. It was found that hybrid active–passive damping allows to increase damping of the first and third modes while preventing instability of uncontrolled ones. Analysis of viscoelastic material thickness variation showed that modal damping distribution can be optimized by proper choice of this parameter. In this particular case, thin cores yielded better active and passive overall performances.

Application to the analysis of other active–passive damping constructions such as active constrained layer damping (ACLD) [7] and active control with passive constrained layer damping (AC/PCLD) variations has been also conducted in order to assess the various hybrid active–passive configurations proposed in the literature. Also, comparison of the performance of several control algorithms has being carried out [8] and analysis of the viscoelastic material temperature-dependence effect on the control performance was presented in Reference [9].

ACKNOWLEDGEMENTS

Support of the “Délégation Générale pour l’Armement”—Advanced Materials Branch, under contract D.G.A./D.S.P./ S.T.T.C./MA. 97-2530, is gratefully acknowledged. The first author acknowledges also the support of the Brazilian government (CAPES) through a doctoral scholarship award.

REFERENCES

1. Trindade MA, Benjeddou A, Ohayon R. Finite element modelling of hybrid active–passive vibration damping of multilayer piezoelectric sandwich beams. part 1: Formulation. *International Journal for Numerical Methods in Engineering* 2001; **51**(7):835–854.

2. Krommer M, Irschik H. On the influence of the electric field on free transverse vibrations of smart beams. *Smart Materials Structure* 1999; **8**(3):401–410.
3. Saravanos DA, Heyliger PR. Coupled layerwise analysis of composite beams with embedded piezoelectric sensors and actuators. *Journal of Intelligent Material Systems and Structures* 1995; **6**(3):350–363.
4. Yildirim V, Sancaktar E, Kiral E. Free vibration analysis of symmetric cross-ply laminated composite beams with the help of the transfer matrix approach. *Communications in Numerical Methods in Engineering* 1999; **15**(9):651–660.
5. Wang G, Wereley NM. Frequency response of beams with passively constrained damping layers and piezo-actuators. In *Smart Structures and Materials 1998: Passive Damping and Isolation*, vol. 3327, Davis LP (ed.), SPIE: Bellingham (USA), 1998; 44–60.
6. van Nostrand WC, Inman DJ. Finite element model for active constrained layer damping. In *Active Material and Smart Structures* vol. 2427, Anderson GL, Lagoudas DC (eds), SPIE, 1995; 124–139.
7. Trindade MA, Benjeddou A, Ohayon R. Modeling of frequency-dependent viscoelastic materials for active–passive vibration damping. *Journal of Vibration and Acoustics* 2000; **122**(2):169–174.
8. Trindade MA, Benjeddou A, Ohayon R. Piezoelectric active vibration control of sandwich damped beams. *Journal of Sound and Vibration* 2000, to appear.
9. Trindade MA, Benjeddou A, Ohayon R. Finite element analysis of frequency- and temperature-dependent hybrid active–passive vibration damping. *Revue Européenne des Éléments Finis* 2000; **9**(1-3):89–111.